
This is an electronic reprint of the original article.
This reprint may differ from the original in pagination and typographic detail.

Levchuk, Irina; Homola, Tomáš; Singhal, Gaurav; Rueda-Márquez, Juan José; Vida, Július; Souček, Pavel; Svoboda, Tomáš; Villar-Navarro, Elena; Levchuk, Olga; Dzik, Petr; Lähde, Anna; Moreno-Andrés, Javier

UVA and solar driven photocatalysis with rGO/TiO₂/polysiloxane for inactivation of pathogens in recirculation aquaculture systems (RAS) streams

Published in:
Chemical Engineering Journal Advances

DOI:
[10.1016/j.ceja.2022.100243](https://doi.org/10.1016/j.ceja.2022.100243)

Published: 15/05/2022

Document Version
Publisher's PDF, also known as Version of record

Published under the following license:
CC BY-NC-ND

Please cite the original version:
Levchuk, I., Homola, T., Singhal, G., Rueda-Márquez, J. J., Vida, J., Souček, P., Svoboda, T., Villar-Navarro, E., Levchuk, O., Dzik, P., Lähde, A., & Moreno-Andrés, J. (2022). UVA and solar driven photocatalysis with rGO/TiO₂/polysiloxane for inactivation of pathogens in recirculation aquaculture systems (RAS) streams. *Chemical Engineering Journal Advances*, 10, Article 100243. <https://doi.org/10.1016/j.ceja.2022.100243>

This material is protected by copyright and other intellectual property rights, and duplication or sale of all or part of any of the repository collections is not permitted, except that material may be duplicated by you for your research use or educational purposes in electronic or print form. You must obtain permission for any other use. Electronic or print copies may not be offered, whether for sale or otherwise to anyone who is not an authorised user.



UVA and solar driven photocatalysis with rGO/TiO₂/polysiloxane for inactivation of pathogens in recirculation aquaculture systems (RAS) streams

Irina Levchuk^{a,*}, Tomáš Homola^b, Gaurav Singhal^c, Juan José Rueda-Márquez^a, Július Vida^b, Pavel Souček^b, Tomáš Svoboda^d, Elena Villar-Navarro^e, Olga Levchuk^f, Petr Dzik^d, Anna Lähde^a, Javier Moreno-Andrés^e

^a Fine Particle and Aerosol Technology Laboratory, Department of Environmental and Biological Sciences, University of Eastern Finland, P.O. Box 1627, Kuopio, 70211 Finland

^b Department of Physical Electronics, Faculty of Science, Masaryk University, Kotlářská 267/2, Brno, 611 37 Czech Republic

^c Department of Chemical and Metallurgical Engineering, School of Chemical Engineering, Aalto University, Kemistintie 1, P.O. Box 16100, Espoo, Aalto, FI-00076 Finland

^d Faculty of Chemistry, Brno University of Technology, Purkyňova 118, Brno, 612 00 Czech Republic

^e Department of Environmental Technologies, Faculty of Marine and Environmental Sciences. INMAR-Marine Research Institute, CEIMAR- International Campus of Excellence of the Sea. University of Cadiz, Spain

^f Institute of Biomedical Systems and Biotechnology, Peter the Great St.Petersburg Polytechnic University, Polytechnicheskaya 29, Saint-Petersburg, Russia

ARTICLE INFO

Keywords:

Photocatalysis
Flexible thin films
Aquaculture water
Bacteria inactivation

ABSTRACT

In this study TiO₂/polysiloxane(SiBi) thin films modified with different concentrations of graphene oxide (GO) were prepared by ink-jet printing on flexible polyethylene terephthalate (PET) substrates. Prepared coatings were characterized by means of scanning electron microscopy (SEM), transmission electron microscopy (TEM), X-ray photoelectron spectroscopy (XPS), ultraviolet photoelectron spectroscopy (UPS), Raman and water contact angle measurements. During photocatalytic tests strong change of color of prepared coatings modified with GO was observed. XPS analysis of thin films after photocatalytic tests suggests that reduction of GO took place. Prepared coatings were studied for inactivation of microorganisms naturally occurring in aquaculture water under UVA and natural solar irradiation. Effect of rGO concentration in prepared coating on inactivation of target bacteria *Aeromonas hydrophila* and *Citrobacter gillenii* was evaluated under UVA irradiation. *Aeromonas hydrophila* was more sensitive to photocatalytic inactivation in comparison with *Citrobacter gillenii*. Higher photocatalytic inactivation of target microorganisms was attributed to thin films with concentration of rGO 1 and 5%. The rGO/TiO₂/SiBi 5% were further tested for inactivation of *Aeromonas salmocida*, *Serratia fonticola strain* and *Lactococcus lactis strain* under natural solar light. Solar photocatalysis slightly enhanced inactivation of *Aeromonas salmocida* and *Serratia fonticola strain*, while opposite was observed for *Lactococcus lactis strain*.

1. Introduction

Fish is considered as an important source of animal protein for human consumption. For instance, in 2017 about 17% of global population consumption of animal protein corresponded to fish-based proteins [1]. Aquaculture is rapidly developing sector in food industry [2]. Thus, 46% to the total global fish production and 52% of fish for global human consumption was attributed for aquaculture in 2018 [1]. Taking into account environmental aspects of the fish production using fish

farms, it was reported that carbon footprint of the farmed fish is about 87% lower than that of beef production [3]. Moreover, it was suggested that Recirculating Aquaculture Systems (RAS) can be considered as a prospective adaptation strategy in the light of climate change and its potential effect on fish production [4]. High yield, relatively low environmental impact and low water use can be mentioned among main advantages of RAS.

In RAS systems, often more than 90% of water is reused [5]. This can be seen as an advantage, however, water reuse in RAS cause elevated

* Corresponding author.

E-mail address: irina.levchuk@uef.fi (I. Levchuk).

<https://doi.org/10.1016/j.cej.2022.100243>

Received 31 October 2021; Received in revised form 24 December 2021; Accepted 7 January 2022

Available online 14 January 2022

2666-8211/© 2022 The Authors.

Published by Elsevier B.V. This is an open access article under the CC BY-NC-ND license

(<http://creativecommons.org/licenses/by-nc-nd/4.0/>).

concentrations of nutrients, organic matter and undesired microorganisms including pathogens in water [6, 7]. The presence of pathogens in RAS water is associated with high risk of infection in reared organisms. To avoid undesirable bacteria in RAS water, disinfection procedures are currently applied, including chlorination [8], UVC disinfection [9], disinfection with peracetic acid [10] and/or hydrogen peroxide [11, 12] and ozonation [13]. However, possible toxic effect of disinfectants on reared organisms [14], cost of chemicals and energy costs [15] are potential challenges associated with abovementioned disinfection methods.

Advanced Oxidation Processes (AOPs) are considered as alternative to conventional water treatment processes, which can be successfully applied for water disinfection and decontamination of organic pollutants [16–21]. Photocatalysis is one of the most widely studied AOP for water and wastewater disinfection [22–28] and it has gained extensive attention in last decades as a promising option for the development of environmentally friendly technologies, especially by taking advantage of the UV-solar spectrum. The most widely studied photocatalyst for decomposition of harmful organic compounds and disinfection of water/wastewater is titanium dioxide (TiO₂). Relatively low cost and high photocatalytic activity are among main advantages of TiO₂ [29, 30].

Composite materials containing TiO₂ and graphene-based structures have attracted significant attention of researchers for application in water and wastewater treatment including photocatalytic disinfection due to unique properties of graphene-based nanomaterials [31, 32]. Various studies have been performed with TiO₂/graphene-based nanocomposites for inactivation of waterborne pathogens [32]. In majority of these studies target microorganism was *Escherichia coli* (*E. coli*), but other microorganisms such as *Staphylococcus aureus*, *Pseudomonas aeruginosa*, *Rhodopseudomonas palustris*, *Enterococcus faecalis*, *Vibrio cholera*, *Staphylococcus aureus*, *Candida*, Fungal cells, etc. were also studied [32]. Thus, enhanced photocatalytic inactivation of *E. coli* under natural solar light was reported when TiO₂-reduced graphene oxide (rGO) was used in comparison with TiO₂, while inactivation rate of *Fusarium solani* spores was similar for TiO₂-rGO and P25 [33]. It should be mentioned that a delay in *E. coli* photocatalytic inactivation was observed with TiO₂ when major part of solar UVA was cut-off ($\lambda > 380$ nm), while it was not the case with TiO₂-rGO [33], which suggests that TiO₂-rGO can be used the near-visible/visible region of the solar spectrum. Moreira et al. [34] have reported that heterogeneous photocatalysis with TiO₂-GO composite was more efficient in comparison with TiO₂ for photocatalytic inactivation of total and resistant populations of fecal coliforms present in urban wastewater under natural solar light. Karaolia et al. 2018 reported similar inactivation rates for *E. coli* in real urban wastewater effluents under simulated solar light for TiO₂ (Aeroxide P25) and TiO₂-rGO, while the lower regrowth was reported for the latter [35]. In another study *E. coli* inactivation by solar photocatalysis with TiO₂/rGO was reported to be strongly dependant on reduction rate of GO [36].

As it can be seen above, majority of studies on photocatalysis with TiO₂ modified with graphene-based structures are focused on disinfection of wastewater and surface waters. Moreover, in majority of abovementioned studies, TiO₂ modified with graphene-based structures is used in form of nanoparticles. However, not many practical applications are existing nowadays for water/wastewater treatment by photocatalysis (in slurry form) due to difficulties arising when photocatalyst (in form of nanoparticles) should be separated from treated water/wastewater [37, 38]. Hence, deposition of photocatalyst on various types of substrates is often used to simplify separation process and ensure absence of nanoparticles in water/wastewater after treatment. Moreover, immobilization could decrease the operation costs of photocatalysis. It should be noted that in some cases photocatalytic activity of immobilized photocatalyst can be equal to that of photocatalyst in form of nanoparticles [39].

Only a few studies have been reported on aquaculture water disinfection by photocatalysis where photocatalyst was used in immobilized

form [16, 17, 40–42]. Hence, the main goal of this work was to evaluate photocatalytic activity of TiO₂ thin films modified with graphene oxide reduced during photocatalysis (rGO) deposited on flexible substrate, which implies a scientific advance from a technological development and water application point of view. Effect of rGO concentration in the thin films was assessed based on the photocatalytic inactivation of microorganisms. In order to consider the complex interactions between water matrix constituents and the reactive species formed in photocatalytic process [43], a real RAS stream was used in this work and naturally occurring bacteria were employed as a target of photocatalytic inactivation.

2. Materials and methods

2.1. Sampling, physico-chemical and microbiological characterization of recirculation aquaculture streams

Experiments in this study were performed with real RAS stream water, collected from Laukaa fish farm (Finland). Detailed description of RAS system layout can be found elsewhere [17, 44]. Sampling was performed after the fish tank and before water treatment units. Water samples were received at our laboratories in coolbox and were kept refrigerated in darkness at 4 °C until experimentation always performed during the first 24 – 72 h. Total ammonia nitrogen, nitrite and nitrate (Procedure 8038 Nessler, LCK341/342, LCK340) as well as alkalinity (ISO 9963–1:1994, TitraLab AT1000, Hach, Loveland, USA) were measured. The pH and conductivity were determined by means of ino-Lab 7110 pH-meter and conductivity meter Orion 101, respectively. The total organic carbon (TOC) concentration was determined using TOC-V_{CSH} analyzer (Shimadzu, Japan) in non-purgeable organic carbon (NPOC) mode. Main physico-chemical characteristics of RAS water are summarized in Table 1.

Collected RAS stream water was microbiologically characterized as received in order to select microorganisms for disinfection efficiency evaluation. Quadrant streak technique was applied for isolation and purification of naturally occurring cultivable bacteria in RAS stream water. Commercial selective agar-based media, namely, Slanetz & Bartley Agar (Panreac), Chromogenic Collinstant Agar (Scharlab) and Thiosulfate Citrate Bile Salts Sucrose Agar (TCBS, Pronadisa, Condalab) were used for this purpose. Petri dishes with TCBS and Chromogenic Collinstant Agar were incubated 24 h at 35 ± 2 °C, while 48 h incubation period was applied for those with Slanetz & Bartley Agar. Colonies isolated on different agars were identified to species by means of amplification and sequentiation of a fragment of 16R rDNA as described elsewhere [45]. Bacterial strains detected were *Aeromonas salmonicida*, *Aeromonas hydrophila*, *Bacillus halotolerans*, *Serratia fonticola*, *Citrobacter gillenii* and *Lactococcus lactis*.

Considering that initial concentration of these microorganisms in RAS stream water was relatively low (10² – 10³ CFU/mL), yeast extract was added to RAS water after which water was kept 24 h at 35 ± 2 °C [16]. This was done in order to increase bacteria concentration and thus secure good statistics and well evaluation of inactivation profiles. The isolation and identification of microorganisms was repeated after addition of the yeast extract. As expected, the types of dominating microorganisms have changed. Thus, colonies isolated from TCBS and

Table 1
Physico-chemical parameters of RAS stream water.

Parameter (unit)	Value
TOC (mg C/L)	13.30 ± 1.90
pH	7.03 ± 0.07
Conductivity (mS/cm)	0.62 ± 0.07
Alkalinity (mg CaCO ₃ /L)	20.80 ± 2.60
NH ₄ ⁺ (mg/L)	0.75 ± 0.10
NO ₂ ⁻ (mg/L)	0.26 ± 0.02
NO ₃ ⁻ (mg/L)	238.3 ± 5.27

Chromogenic Collinstant Agar were identified as *Aeromonas hydrophila* and *Citrobacter gillenii*, respectively and their initial concentration was significantly higher ($\sim 10^7$ CFU/mL). *Aeromonas hydrophila* (*A. hydrophila*) and *Citrobacter gillenii* (*C. gillenii*) were used as target microorganisms for assessing efficiency of UVA-based photocatalytic disinfection of RAS stream. These species are gram-negative, γ -proteobacteria and often found in the intestinal microbiota of fish, which can be associated with fish diseases [46, 47]. Moreover, *Aeromonas* was reported as a fish pathogen and it is of interest for aquaculture sector [2, 48].

In a second round of experimentation (See Section 2.4), experiments at naturally occurring bacterial concentrations were performed with colonies isolated on Slanetz & Bartley Agar, TCBS and Chromogenic Collinstant Agar, which were identified as *Lactococcus lactis strain*, *Aeromonas salmocida* and *Serratia fonticola strain*, respectively.

2.2. Preparation of thin films

The preparation GO/TiO₂/polysiloxane(SiBi) thin films was conducted as described below. The ink was prepared by mixing: i) 24 mL of TiO₂ dispersion (20 wt% of nanoparticulate TiO₂ P-25 nanopowder of <25 nm particle size, 718,467 Sigma Aldrich) in Dowanol® PM (1-methoxypropan-2-ol) with ii) 8 mL of polysiloxane SiBi-0 binder [49] (20 wt% in anhydrous ethanol) with iii) various volume of alkylamine functionalized graphene oxide (2 mg/mL in toluene) (809,055 Sigma Aldrich) and iv) 24 mL of isobutanol. Approx. 45 g of 1 mm glass balls were added to dispersion in a 100 mL glass vial and this was placed on a mixer set to 90 rpm for 8 h. The final GO/TiO₂/polysiloxane(SiBi) ratio was 0, 1, 5, 10 wt.% to TiO₂/polysiloxane(SiBi-0). To maintain the same TiO₂/SiBi-0 concentration in all samples, the samples were top up to same volume with toluene. The GO/TiO₂/polysiloxane(SiBi) films were deposited on polyethylene terephthalate (PET) using bar coater method using bars of wire diameter 30 μ m. The materials and procedures employed for the printable suspension formulation have been reported in detail in our previous work [50].

2.3. Characterization of thin films

The wettability of the GO/TiO₂/polysiloxane(SiBi) surfaces was evaluated by a measurement of the water contact angle (WCA) using SeeSystem (Advex Instruments, Czech Republic). Water droplet with volume of 1 μ l was deposited onto the surface using a micropipette. The images of the droplets for analysis were taken approximately 3 s after the deposition and the average WCA was calculated from approximately 10 measurements.

The surface morphology of coatings was examined by means of a Mira3 scanning electron microscope (Tescan, Czech Rep.). The samples were coated with 20 nm gold. The images, at 50 kx magnification, were captured at an accelerating voltage of 10 kV and a working distance of 10 mm. Presence of GO in samples was confirmed using the transmission electron microscopy (TEM, JEM-2100F, JEOL Ltd.) with acceleration voltage of 200 kV. Prior measurements nanoparticles was scratched from the substrate and dispersed in ethanol using ultrasound.

Further evidence of the nature and extent of the binder mineralization was obtained by X-ray photoelectron spectroscopy (XPS) using an Al K α ESCALAB 250Xi (ThermoFisher Scientific). All samples were measured at one spot (650 μ m) at a take-off angle of 90° in 10⁻⁷ mbar vacuum at 20 °C. An electron flood-gun was used to compensate for charges on sample surfaces. The spectra were referenced to Ti(IV) 2p component at 458.7 eV [51]. Atomic concentration was determined from wide spectra measured from two spots. The Shirley background shape was used and the components used for the peak deconvolutions were mixed Gauss-Lorentzian lines (70% Gaussian and 30% Lorentzian).

Ultraviolet photoelectron spectroscopy (UPS) with He I (21.22 eV) was employed to calculate work function of the coatings by subtracting binding energy at the SE cut-off from the energy of the incident light.

Furthermore, the coatings were analyzed with Horriba LabRAM HR Evolution microRaman spectrometer with 532-nm laser to observe crystalline structure of anatase-TiO₂ along with presence of GO.

2.4. Experimental procedures for photocatalytic disinfection tests

2.4.1. UVA-based photocatalytic disinfection

The photocatalytic disinfection tests were performed in batch mode at ambient temperature (22 ± 2 °C). Prepared photocatalytic coatings (geometrical surface area of 25 cm²) were located in borosilicate Petri dish filled with 20 mL of RAS water (after addition of yeast) and irradiated using LEDs ($\lambda = 370$ nm). First 15 min of each photocatalytic test was performed in absence of light, after which LEDs were switched on. The UVA intensity was measured using UV AB Light Meter (General UV513AB). It should be noticed that an error coefficient was calculated and applied to measurements of UV AB Light Meter. The intensity of UVA on the surface of the water was 48 ± 0.7 W/m². Constant magnetic stirring was applied during all experiments. Samples were collected at desired time intervals and microbiologically analyzed. Initial samples were microbiologically analyzed before each experiment, in order to quantify the initial concentration of bacteria (CFU/mL). Control tests (in absence of photocatalyst; in absence of UVA) were also conducted. The TOC values were measured before and after each test. Concentration of *Aeromonas hydrophila* and *Citrobacter gillenii* were monitored (See Section 2.1) on the course of experiments by standard plate counts. Results of *A. hydrophila* and *C. gillenii* inactivation were represented in a form of Log (N/N₀) as a function of contact time and UVA dose. The UVA dose (D_{UVA}) was calculated as shown in Eq. (1).

$$D_{UVA} = D_{t-1} + I_t \cdot \Delta t \quad (1)$$

Where I_t is the intensity of UVA irradiation (W/m²) and Δt is sampling time interval (h).

The detection limits (D.L.) for *A. hydrophila* and *C. gillenii* inactivation during UVA-based photocatalytic tests were 10 CFU/mL, which corresponds to 5.9 – 6.15 decimal log reductions taking into consideration relatively high initial concentration of microorganisms ($\sim 10^7$ CFU/mL).

2.4.2. Solar driven photocatalytic disinfection

Solar photocatalytic disinfection tests were performed using real RAS stream water (yeast was not added, see Section 2.1) received the same day under ambient temperature (38 ± 2.3 °C). Experiments were conducted in Finland under natural solar irradiation during summer sunny days. Two identical glass reactors (total volume 1200 mL) filled with 1000 mL of RAS water were used for experiments. Photocatalytic films were attached to the walls and bottom of the glass reactor used for photocatalytic tests as reported elsewhere [16]. The geometrical area of photocatalyst was 0.54 cm²/mL. Another identical reactor (without photocatalyst) was used for SODIS as a reference/blank test. Solar photocatalysis and SODIS tests were performed under constant magnetic stirring during 180 min. As in Section 2.4.1, samples were collected at desired time intervals and microbiologically analyzed by means of standard plate counts. Here, the low initial bacterial concentration implies the plating of larger volumes of water to increase detection limit of samples. Thus, membrane filtration was applied to adequately monitor concentration of target microorganisms (*Aeromonas salmocida*, *Serratia fonticola strain* and *Lactococcus lactis strain*). Water samples were collected at 0, 30, 60, 90, 120 and 180 min.

The UVA + UVB intensity was measured using UV AB Light Meter (General UV513AB). The average UVA + UVB intensity on the surface of the water during solar experiments was 24 ± 7 W/m². The cumulative UV Dose (Q_{UV} , Wh/m²) was calculated according to Eq. (2).

$$Q_{UV,t} = Q_{UV,t-1} + \sum (UV_i \cdot \Delta t) \quad (2)$$

Where $Q_{UV,t}$ - the cumulative UV radiation dose received at each instant

(Wh/m^2), UV_t – radiation intensity measured at certain time intervals (W/m^2), Δt – time interval between measurements (h).

In case of solar photocatalytic disinfection the D.L. for *Aeromonas salmonicida*, *Serratia fonticola*, and *Lactococcus lactis* strains was 2 CFU/mL, which corresponds to 2.5–2.8, 2.7–2.8, and 1.05–1.87 decimal log reduction, respectively. Lower D.L. in solar driven tests can be attributed to lower initial concentration of microorganisms ($\sim 10^2$ – 10^3 CFU/mL).

3. Results and discussion

3.1. Characterization of prepared thin films

Prepared coatings were extensively characterized before photocatalytic tests. The morphology of GO/TiO₂/polysiloxane(SiBi) coatings of different amount of GO (0%, 1%, 5%, 10%) can be observed from SEM images presented in Fig. 1.

As shown in Fig. 1, the structure of all coatings is very similar with high homogeneity and mesoporosity. The difference can be observed for coatings with GO concentration 5% and 10%. The SEM images indicate the presence of GO sheets on the surface of the coatings. From TEM images of coatings before photocatalytic tests shown in Fig. 2 presence of GO is obvious in all samples except for film with 0% of GO.

Thickness of prepared coatings was measured. The profilometric scans of TiO₂/SiBi coatings with various amount of GO and mean thickness of prepared coatings are shown in Fig. 3.

As can be seen from Fig. 3, mean thickness of films doped with 5%

and 10% of GO was higher in comparison with GO 1% and 0%. It should be noted that for comparison of photocatalytic activity of thin films, thickness should be within the same range as it may affect the mean areal loading of TiO₂ [52].

Table 2 shows the water contact angles for GO/TiO₂/polysiloxane (SiBi) coatings of different amount of GO (0%, 1%, 5%, 10%). The reference sample with 0% of GO showed considerably high water contact angle of $92.5^\circ \pm 3.2^\circ$ indicating hydrophobic nature of the coating. Addition of 1%, 5% and 10% of GO in TiO₂/polysiloxane(SiBi) lead to slight decrease of water contact angle, leading to values of $91.2^\circ \pm 2.5^\circ$, $82.9^\circ \pm 3.3^\circ$ and $80.6^\circ \pm 2.6^\circ$, respectively. The decrease in water contact angle and improvement in wettability is clearly associated with presence of GO and its various functional groups such as epoxy, hydroxyl, and carboxyl. This result is in the scope with our previous study on TiO₂/polysiloxane(SiBi) films [45] in which the hydrophilicity was tailored by ambient air plasma treatment. The plasma treatment shows much more efficient for wettability improvement as the water contact angle decreases to $11.9^\circ \pm 0.8$ which was accompanied by rapid absorption of water into the coating. On the other hand, the excellent hydrophilicity was not beneficial for bacteria inactivation in drinking and seawater, possibly due to slightly lower adhesion of these bacteria to the hydrophilic surface of photocatalytic film, which in turn may decrease the efficiency of photocatalytic response of the coating [45].

Atomic concentrations of elements detected on the surface of GO/TiO₂/polysiloxane(SiBi) films deposited on Si wafer are presented in Fig. 4a. The surface of the sample with 0% GO showed 25 at.% of carbon,

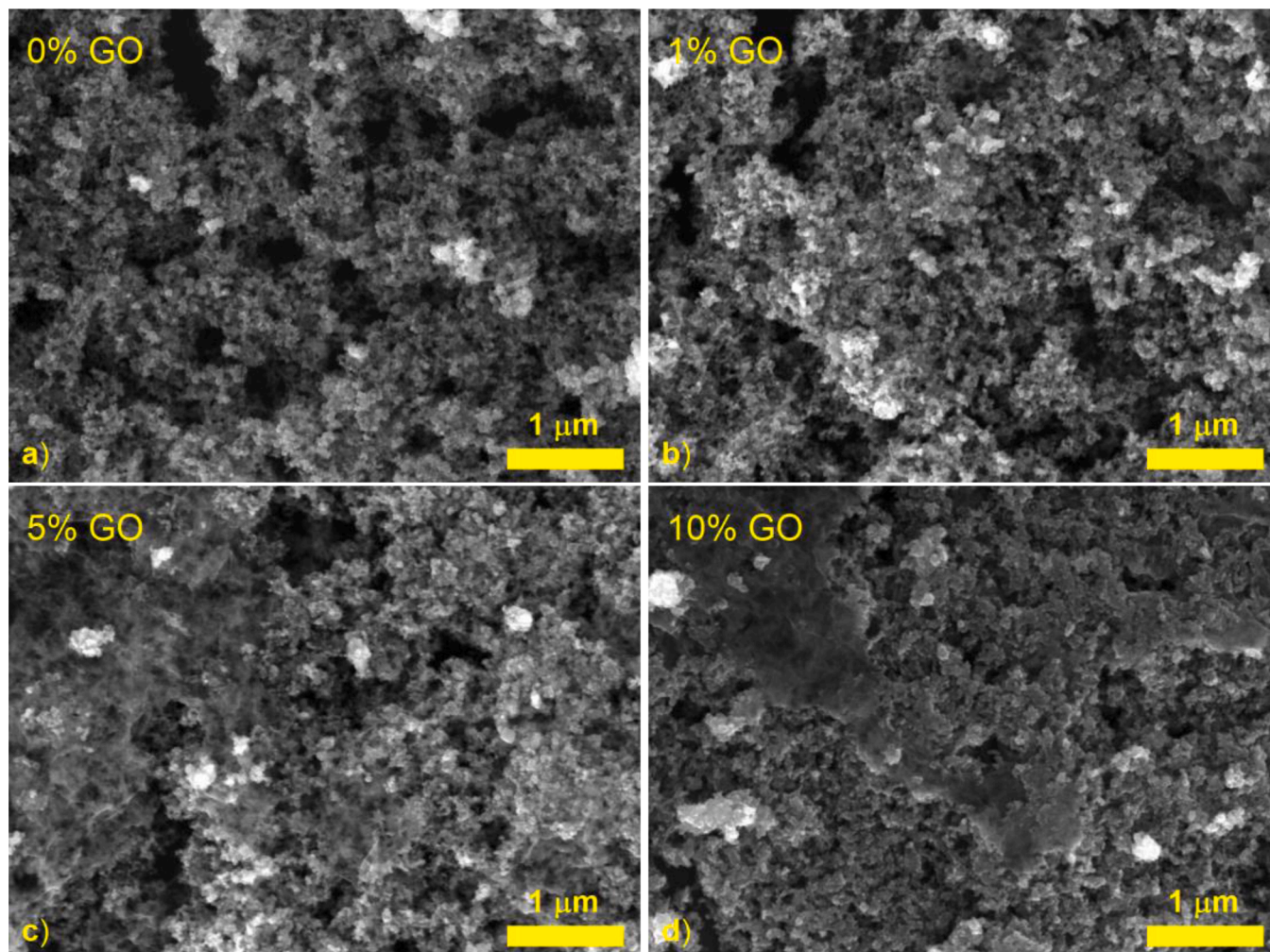


Fig. 1. SEM images of GO/TiO₂/polysiloxane(SiBi) thin films before photocatalytic tests.

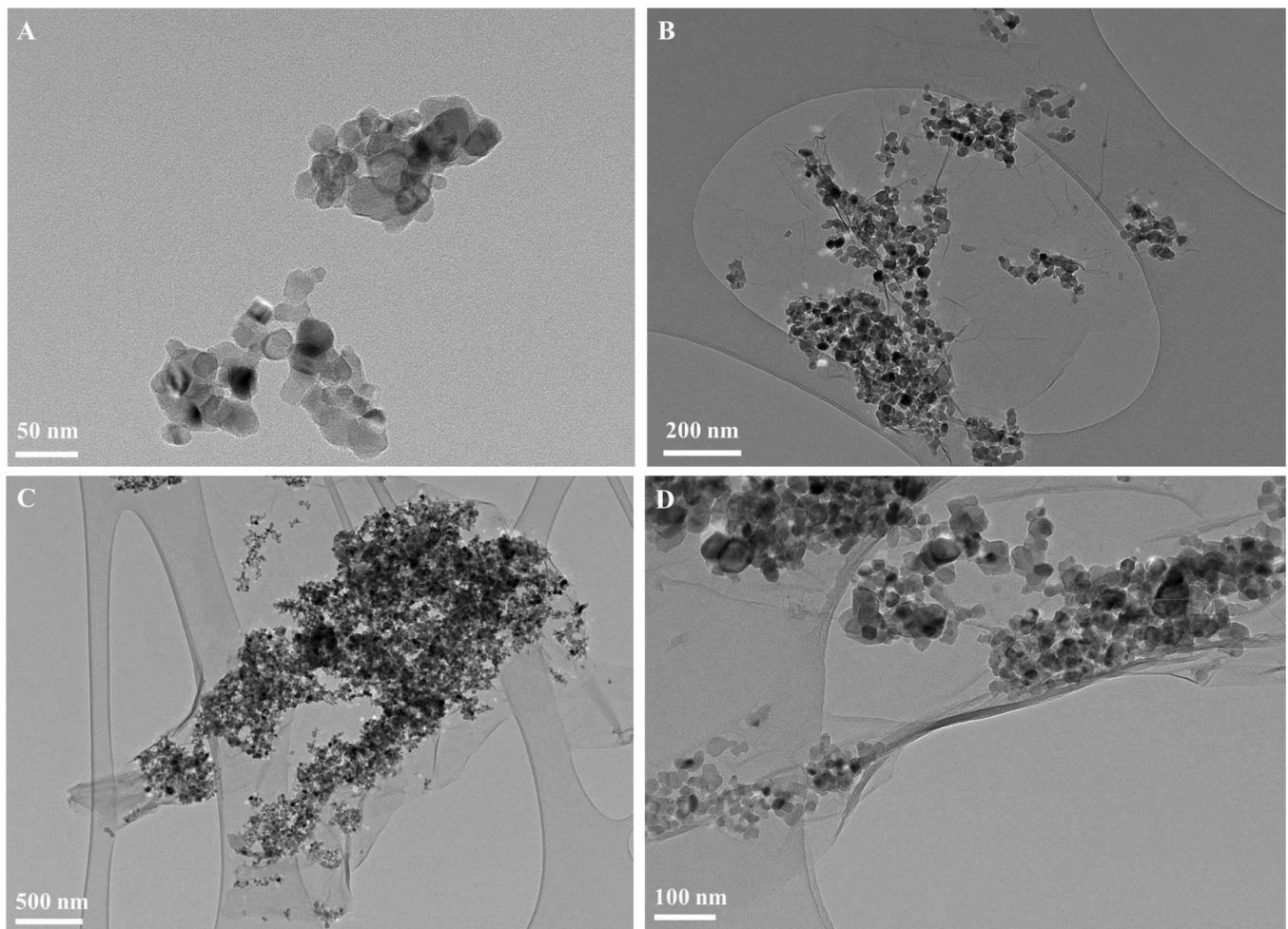


Fig. 2. TEM images of GO/TiO₂/polysiloxane(SiBi) thin films before photocatalytic tests. A – 0% GO, B – 1% GO, C – 5% GO, D – 10% GO.

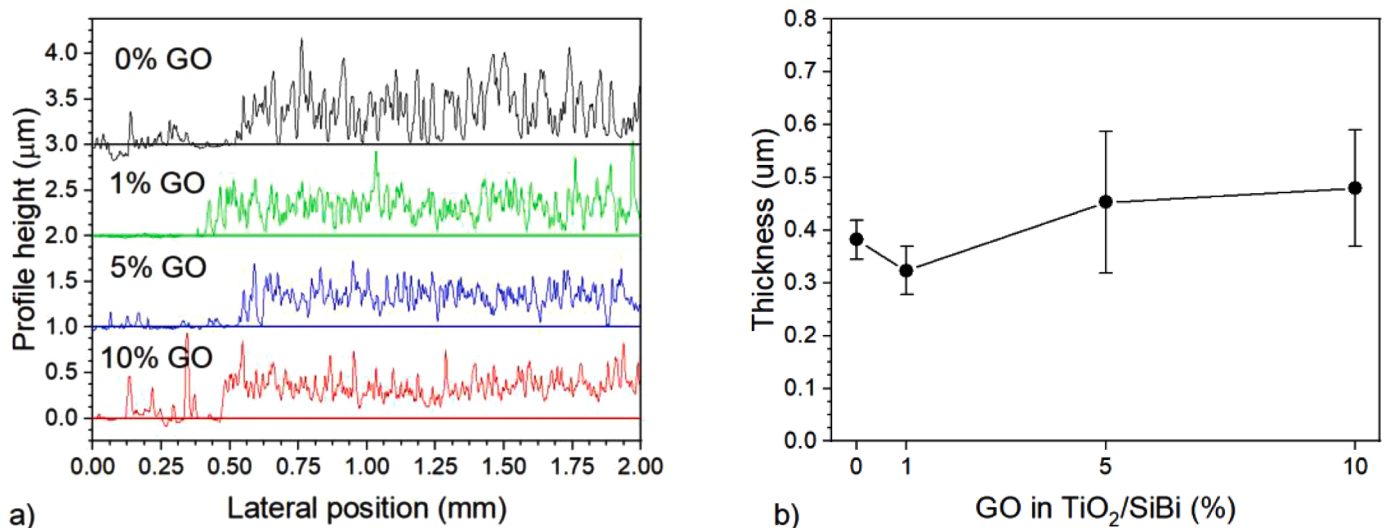


Fig. 3. a) Profilometric scans of TiO₂/SiBi coatings with various amount of GO and b) Average thickness of TiO₂/SiBi coatings with various amount of GO.

which can be attributed to the organic part (methyl groups) of the organosilica binder (SiBi) along with surface contamination possibly present due to the adsorption of hydrocarbons from ambient air. The 45.1 at.% of oxygen detected on the surface includes contributions from TiO₂ nanoparticles, oxygen bound to silicon in the SiBi and oxygen

bound to carbon in the surface contaminants. The silicon and titanium concentrations were 24 at.% and 5.7 at.%, respectively. Addition of 1% of GO in TiO₂/polysiloxane(SiBi) had no considerable effect on surface chemistry and atomic concentrations detected by XPS remained the same within the statistical error. However, with 5% GO in TiO₂/

Table 2

Water contact angle of GO/TiO₂/polysiloxane(SiBi) thin films before photocatalysis.

Concentration of GO in TiO ₂ /SiBi	Water Contact Angle
0%	92.5° ± 3.2°
1%	91.2° ± 2.5°
5%	82.9° ± 3.3°
10%	80.6° ± 2.6°

polysiloxane(SiBi), the atomic concentration of carbon increased to 43.9 at.%, whereas the concentrations of oxygen, silicon and titanium decreases accordingly. For the sample with 10% GO in TiO₂/polysiloxane (SiBi), the atomic concentration of carbon increased to 53.6 at.% accompanied with further decrease of oxygen, silicon and titanium concentrations. The C:O ratio increase from 0.56 for sample with 0% of GO to 1.50 for the sample with 10% of GO.

The high-resolution XPS spectra in the C 1 s and O 1 s regions were analysed in order to discuss the changes in the bonding states of carbon and oxygen induced by the addition of various GO concentration (1%, 5%, 10%) in GO/TiO₂/polysiloxane(SiBi) coatings. The high-resolution C 1 s peaks for samples of different amount of GO (0%, 1%, 5%, 10%) are shown in Fig. 4b. The sample without GO displayed a pronounced peak at around 284.5 eV, corresponding to the Si—CH₃ groups from the polysiloxane SiBi binder. This component was observed previously in

similar siloxane coatings [53–55]. This peak overlaps with the C—C peak from surface contamination at around 284.8 eV. Furthermore, the carbon in surface contamination can be in a form of C—OH, C = O and O—C = O bonds contributing to the signal in the C 1 s region at around 286.3 eV, 287.8 eV and 288.8 eV, respectively. A typical XPS spectrum in the C 1 s region of GO consists of four components. The carbon in the C—C bonds in the graphene lattice, the carbon bound to a hydroxide C—OH or ethers C—O—C, carbonyl carbon in C = O and carbon in carboxyl groups O—C = O [56–58]. These components contribute to the signal at the same binding energy as the corresponding bonds in the surface contaminants. The C—C component can be further broken down into two components at 284.9 eV and an asymmetric peak at 284.4 eV corresponding to sp³ and sp² hybridization, respectively. Because of the number of components present in a narrow C 1 s region and a lack of possible constraints, the deconvolution of the XPS spectra of such complicated surface would be too ambiguous. Qualitatively, Fig. 4b shows mostly unchanged structure of the C 1 s region for the sample with 1% GO compared to the sample without GO, with a slight increase around 288.0 eV where the C = O component typically occurs. With addition of 5% GO into the film the signal from C—C component increased. Similarly, the signal from the oxygen-containing functional groups increased. A further increase of these components was detected on the surface of the sample with 10% GO.

The high-resolution O 1 s peaks for samples of different amount of

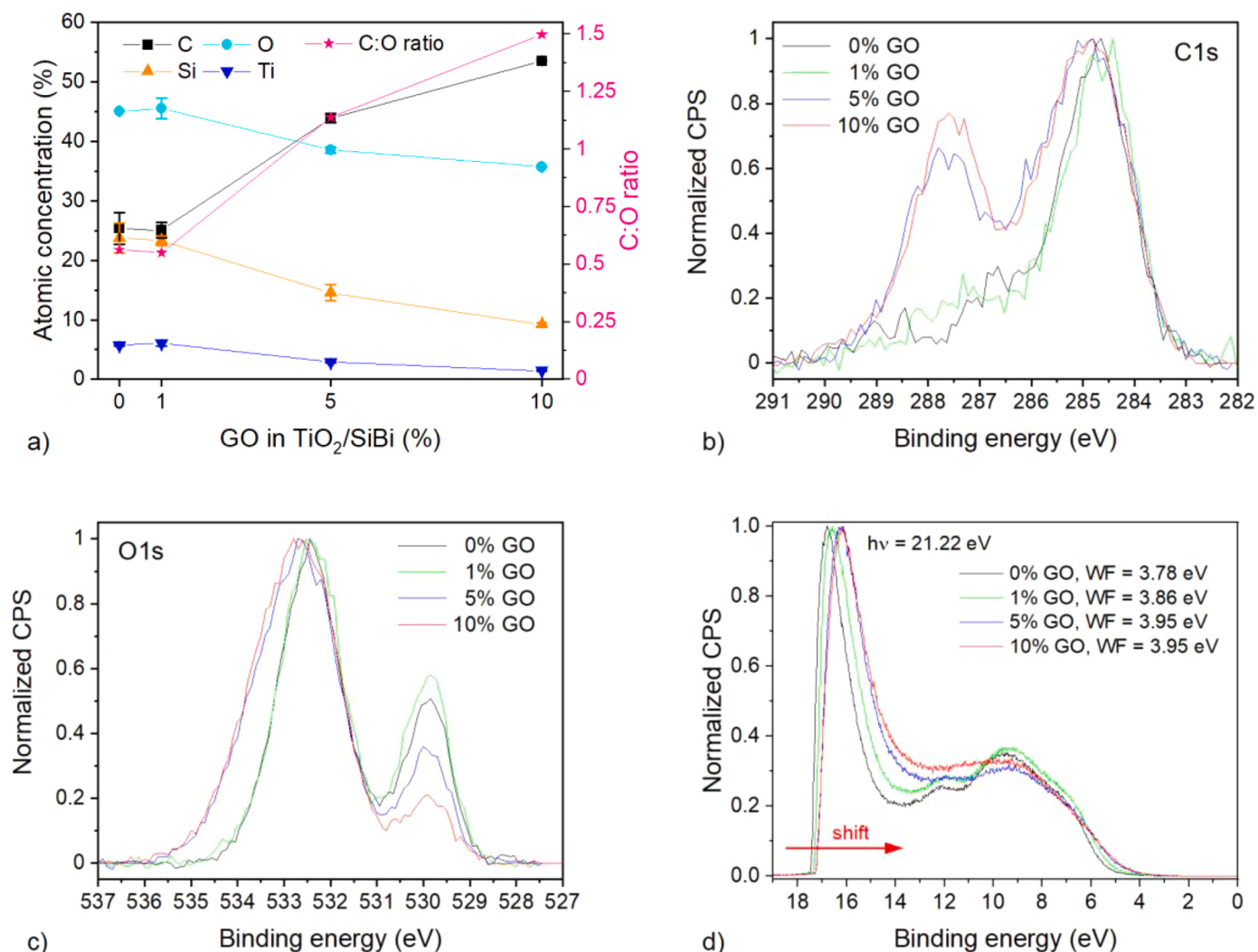


Fig. 4. XPS and UPS spectra of GO/TiO₂/polysiloxane(SiBi) thin films before photocatalytic tests: a) atomic concentrations of elements detected on the surface of the films; b) high resolution C1s peaks in XPS spectra; c) high resolution O1s peaks in XPS spectra; d) the UPS spectra of the films.

GO (0%, 1%, 5%, 10%) are presented in Fig. 4c. The sample without GO displayed two pronounced peaks at around 530.0 eV and 532.5 eV, corresponding to oxygen bound to titanium in TiO₂ and oxygen bound to silicon in SiBi, respectively. The second peak is shifted to lower binding energies compared to the typical value of SiO₂ at 532.9 eV due to one methyl group bound to the silicon atom instead of oxygen in the SiBi [54, 59]. There was no significant change observed for the structure of the peaks by adding 1% GO to the film. After adding 5% GO the components corresponding to oxygen bound to carbon in C = O, C—OH and C—O—C environments increased. The positions of these peaks varies in the literature but they can be typically found at binding energies around 532.0 eV, 533 eV and 533.8 eV [58, 60]. The relative intensity of the TiO₂ peak decreases with addition of GO.

The UPS spectra for samples of different amount of GO (0%, 1%, 5%, 10%) are shown in Fig. 4d. The secondary cutoff shift indicates a slight increase in work function for samples with increased concentration of GO. The sample without GO showed work function of 3.78 eV, whereas coatings with higher concentrations of GO (1%, 5% and 10%) showed work function of 3.86 eV, 3.95 eV and 3.95 eV. The increase in work function may be associated with presence of GO and presence of various hydrophilic groups in GO.

Raman spectra for samples differing in the amount of GO (0%, 1%, 5%, 10%) in TiO₂/SiBi are presented in Fig. 5. The Raman shift range of 100 cm⁻¹ – 1800 cm⁻¹ is shown in Fig. 5a, while the range of 1800 cm⁻¹ – 3200 cm⁻¹ is represented in Fig. 5b. Both figures differ in the y-scale axis due to low intensities of the second order peaks. The sample with 0% of the graphene oxide shows peaks corresponding to the TiO₂ layer. Low intensity D and G carbon peaks at ~ 1350 cm⁻¹ and 1600 cm⁻¹, respectively, become distinguishable for the sample with 1% of the graphene oxide. Samples with 5% and 10% of graphene oxide show clear D and G carbon peaks at the same positions as the previous sample. Also the 2D peak at ~ 2700 cm⁻¹ ascribed to an out-of-plane graphene oxide vibration mode and the D + G peak sometimes called the 3S peak arising as the second order combination of the D and G peaks are clearly visible [61, 62]. No significant shifts of the observed graphene oxide together with constant ratio of the intensities of the D and G peaks suggest that there is no significant change in the graphene oxide structure and chemistry with differing concentrations of the graphene oxide in TiO₂/SiBi.

3.2. Photocatalytic bacteria inactivation

3.2.1. UVA-based photocatalytic inactivation of *Citrobacter gillenii* and *Aeromonas hydrophila*

The UVA-based photocatalytic disinfection tests were performed with *A. hydrophila* and *C. gillenii* as target microorganisms in RAS water (after addition of yeast). Blank tests (i) in absence of photocatalyst (UVA only) and (ii) in absence of irradiation (photocatalyst only) were conducted. Blank tests with tested photocatalysts in absence of light demonstrated negligible change of *A. hydrophila* and *C. gillenii* concentrations (results are not shown) during 120 min of experimental time, which was equal to that during photocatalytic tests. These results indicate that there was almost no adhesion of *A. hydrophila* and *C. gillenii* to tested photocatalytic films

During photocatalytic disinfection tests (under UVA and solar light) we observed profound changes in color in all coatings containing GO, the strongest color changes were observed for the coating with highest amount of GO (Fig. 6, A and B). In order to understand the nature of observed color changes, we have performed additional XPS analysis of C 1 s peak in the sample with 10% of GO, measured before and after photocatalysis (Fig. 6).

Results presented in Fig. 6 revealed significant changes in the region related to carbon-oxygen bonds and slight changes in C—C main peak, possibly related to shift from sp³ (graphene oxide) towards sp² (graphene) hybridization. Therefore, the photocatalysis can efficiently self-enhance the coating properties by changing the graphene oxide (GO) to reduced graphene oxide (rGO), which apparently contributed to further improvement of decontamination of water. Consulting the scientific literature, photocatalytic reduction of GO in presence of TiO₂ under UV and/or visible light has been reported earlier. For instance, reduction of GO was reported after 15 min of UV irradiation in mixture of TiO₂ nanoparticles and GO in ethanol [63]. Reduction of graphene oxide nanosheets deposited within TiO₂ (anatase) thin films was reported when these films were immersed in ethanol solution and irradiated using mercury lamp (peaks at 275 nm, 350 nm and 660 nm) for 4 h [36]. It should be noted that reduction of GO in presence of TiO₂ and ethanol was also reported under visible light irradiation [64]. Reduction of GO in presence of TiO₂, ethanol and UV light was attributed to scavenging of electron-hole pairs generated during UV irradiation of TiO₂ by ethanol, which leads to production of ethoxy radicals. The latter in turn leads to accumulation of electrons within TiO₂, which interact with GO and reduce functional groups [63]. As far as authors are aware, there were no reports of GO reduction in presence of TiO₂ in water as observed in our study. It should be noted that presence of organic

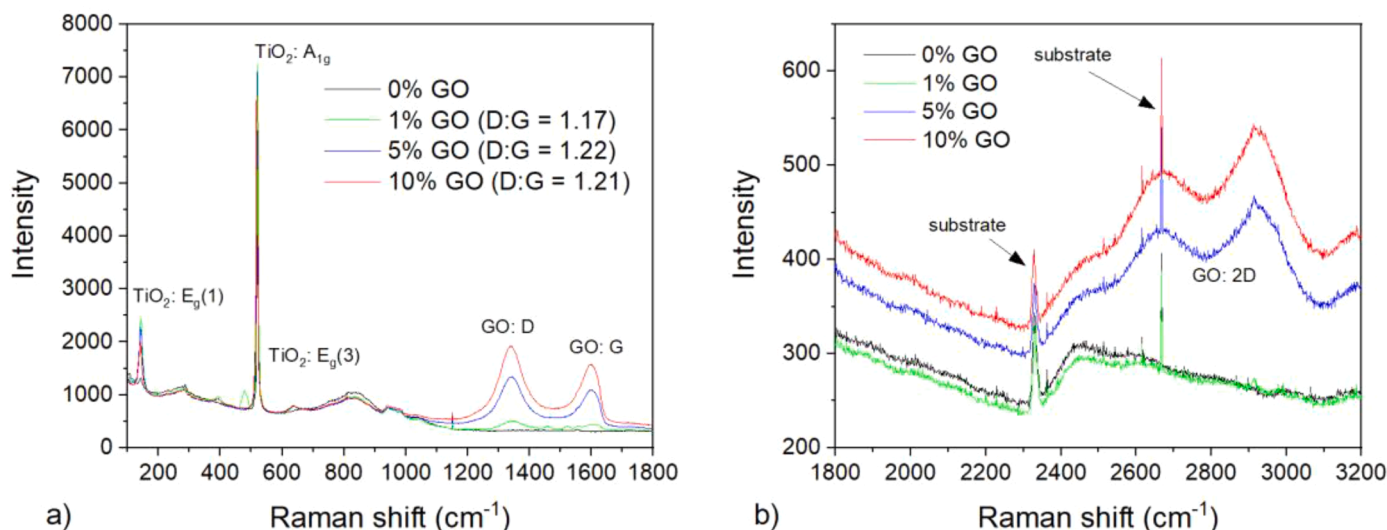


Fig. 5. Raman spectra of GO/TiO₂/polysiloxane(SiBi) thin films before photocatalytic tests.

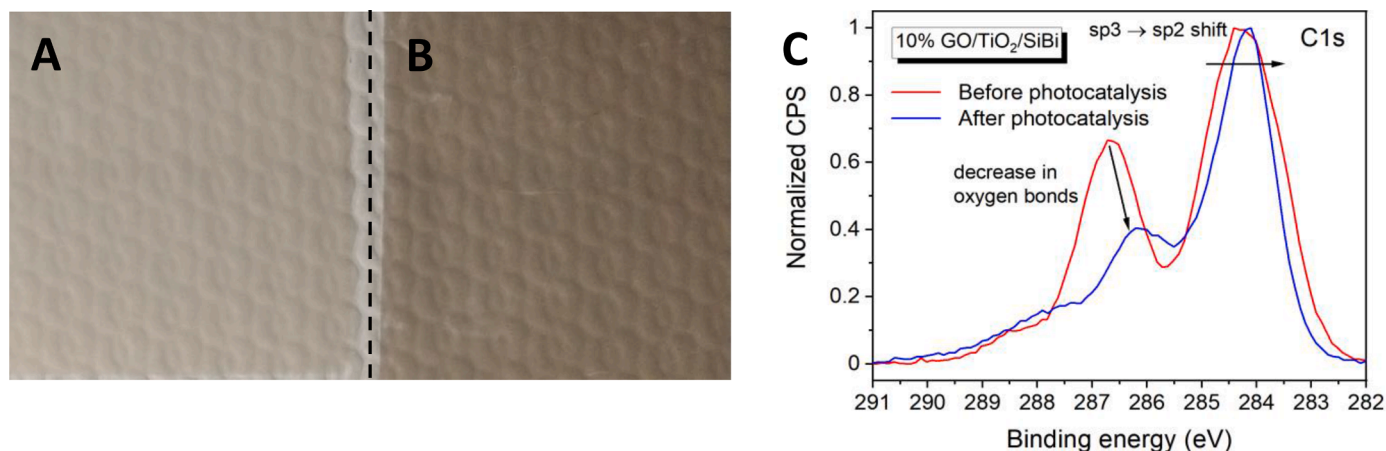


Fig. 6. A – photo of GO/TiO₂/SiBi coating 10% before photocatalytic tests, B – photo of GO/TiO₂/SiBi coating 10% after photocatalytic tests (after 60 min under natural solar light), C – High resolution C1s peaks in XPS spectra of 10% GO/TiO₂/polysiloxane coating deposited on PET foil measured before and after photocatalysis indicating reduction of GO towards rGO.

compounds within prepared GO/TiO₂/SiBi thin films was observed, which could contribute to GO reduction under UVA and solar irradiation.

Results of target bacteria inactivation (log scale) as a function of UV dose are shown in Fig. 7. Both bacteria have shown to be sensitive to UV irradiation, which can be attained to their low ability to survive under stress conditions as opportunistic bacteria. However, it can be noticed from Fig. 7 that *Aeromonas hydrophila* was more sensitive to photocatalytic inactivation than *Citrobacter gillenii*. Inactivation of *A. hydrophila* by UVA-based photocatalysis with TiO₂/SiBi (0% rGO) did not lead to enhancement as compared to UVA only, which can be attributed to competition for the absorption of photons between TiO₂/SiBi (0% rGO) film and bacteria suspended in water [65]. Thus, Sordo et al. [65] have reported decrease of solar-driven photocatalytic inactivation of *E. coli* in water with TiO₂ deposited on reactor wall in comparison with solar disinfection. This was explained by competition between immobilized TiO₂ and bacteria suspension for absorption of photons [65]. However, enhanced inactivation of *A. hydrophila* ATCC 35,654 was reported in a thin-film fixed-bed reactor (P25 Degussa was immobilized) under natural solar light, where the 1.33 log inactivation

was reported for photocatalysis (single pass across reactor, flow rate 4.8 L/h) [41].

Despite the competition for the absorption of photons, TiO₂/SiBi thin films modified with rGO (1, 5 and 10%) showed enhanced inactivation of *A. hydrophila* (Fig. 7A) in comparison with TiO₂/SiBi (0% rGO) and UVA only. These results suggest that TiO₂/SiBi thin films modified with rGO possess higher photocatalytic activity in comparison with TiO₂/SiBi. The estimated UVA dose required to reach 2 LRV and 4 LRV of *A. hydrophila* was quite similar for photocatalysis with TiO₂/SiBi/rGO 1% (6.97 Wh/m² and 15.47 Wh/m², respectively) and rGO/TiO₂/SiBi 5% (7.43 Wh/m² and 18.50 Wh/m², respectively), while higher dose was needed in case of rGO/TiO₂/SiBi 10% (16.42 Wh/m² and 22.03 Wh/m², respectively).

Citrobacter gillenii was more resistant to photocatalytic inactivation. It can be seen from Fig. 7B that presence of photocatalysts enhanced inactivation of *C. gillenii*. Taking into consideration estimated UVA dose required for reaching 2 LRV, the following order can be established starting from the higher photocatalytic performance: rGO/TiO₂/SiBi 5% (2 LRV 9.63 Wh/m²) > rGO/TiO₂/SiBi 1% (2 LRV 17.41 Wh/m²) > TiO₂/SiBi (2 LRV 19.35 Wh/m²) > rGO/TiO₂/SiBi 10% (2 LRV 22.90

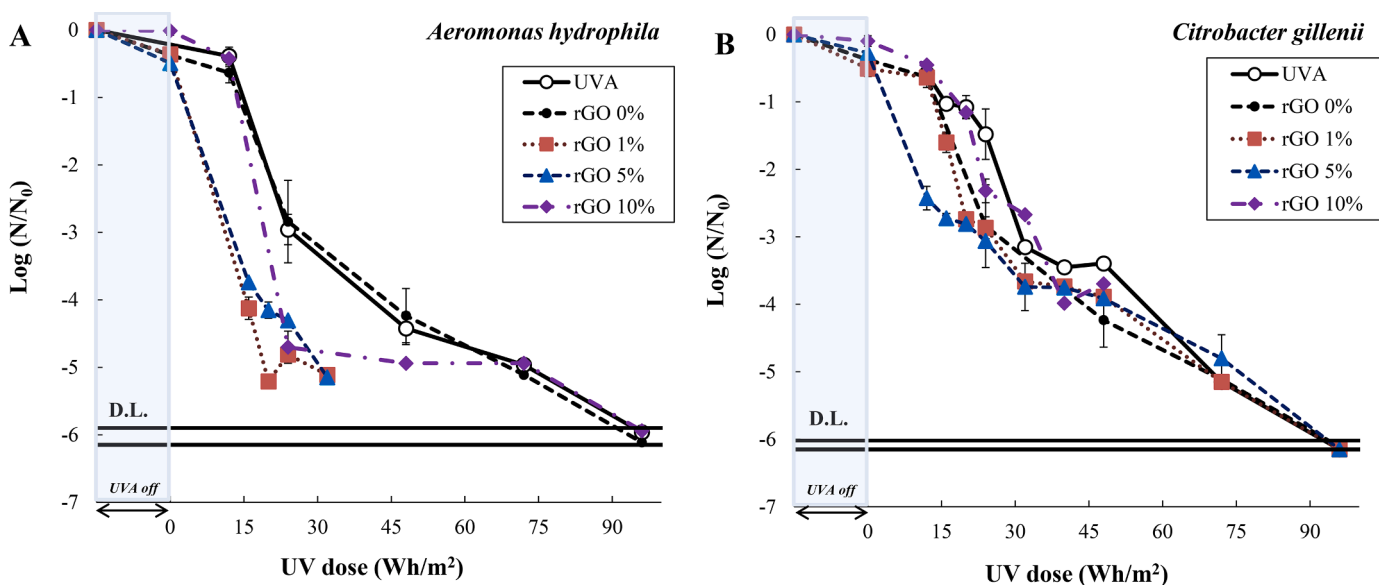


Fig. 7. Inactivation profiles of *Aeromonas hydrophila* (A) and *Citrobacter gillenii* (B) by UVA driven photocatalysis with TiO₂/SiBi composites modified with rGO. Dark period (UVA off) was 15 min.

Wh/m²). However, the UVA dose needed for 4LRV was similar to all thin films modified with rGO (~40 Wh/m²) and slightly higher for TiO₂/SiBi (43.96 Wh/m²). Based on obtained results with *C. gillenii* and *A. hydrophila* it can be suggested that the highest inactivation was observed for TiO₂/SiBi modified with 1 and 5% of rGO. Hence, it was decided to select rGO/TiO₂/SiBi 5% for further experiment as the best among tested. It should be mentioned that concentration of rGO, which was selected in this work was similar to that in studies of Fernandez-Ibanez et al. [33] and Cruz-Ortiz et al. [66], in which TiO₂-rGO (5 w/v %) was reported to be more active for photocatalytic inactivation of *E. coli* than TiO₂. Moreover, photocatalytic activity of TiO₂-rGO under visible light ($\lambda > 420$ nm) has been demonstrated [66]. Similarly, higher photocatalytic activity for inactivation of fecal coliforms in urban wastewater by TiO₂-rGO (4 wt%) in comparison with TiO₂ was reported by Moreira et al. [34]. In order to check if prepared in this study rGO/TiO₂/SiBi 5% films are active under visible light additional tests were conducted with model solution of formic acid in Milli-Q water (experimental set-up and results are shown in Supplementary Materials). No photocatalytic activity under visible light only was not observed ($\lambda > 410$ nm).

Enhanced inactivation of target bacteria by using TiO₂/SiBi films modified with rGO can be possibly attributed to suppressed recombination of charge carriers in TiO₂ due to transfer of electrons through rGO

[32]. Taking into account that GO possess disturbances in sp² bonding network, it acts as electrical insulator. Hence, reduction of GO leads to elimination of oxidized part of GO and enhanced electrical conductivity and fast electron transfer [67].

3.2.2. Solar driven photocatalytic disinfection of real RAS stream water

Solar driven photocatalysis was conducted using rGO/TiO₂/SiBi 5% thin films and real RAS stream water was used. Solar water disinfection (SODIS) was used as reference test. Air and water temperatures were monitored during experiments. Results are shown in Fig. 8.

As can be seen from Fig. 8, presence of rGO/TiO₂/SiBi 5% thin films enhanced inactivation of *Aeromonas salmocida* and *Serratia fonticola strain*, while opposite was observed for *Lactococcus lactis strain*. Detection limits were reached by SODIS and solar photocatalysis for *Aeromonas salmocida* and *Lactococcus lactis strain*. It should be noted that water temperature during SODIS and solar photocatalysis increased from 15 to 29 °C. The well-known synergetic effect of SODIS was reported for inactivation of mesophilic pathogens (e.g. coliforms) when temperature of the water raise above 45 – 55 °C (depending on studied microorganisms) [68–70], which is higher than optimal and maximum temperature of mesophilic bacteria. The optimal temperature for *Aeromonas salmocida*, *Serratia fonticola strain* and *Lactococcus lactis strain* are within the range of 25 – 35 °C [71], 20 – 37 °C [72] and around 30 °C

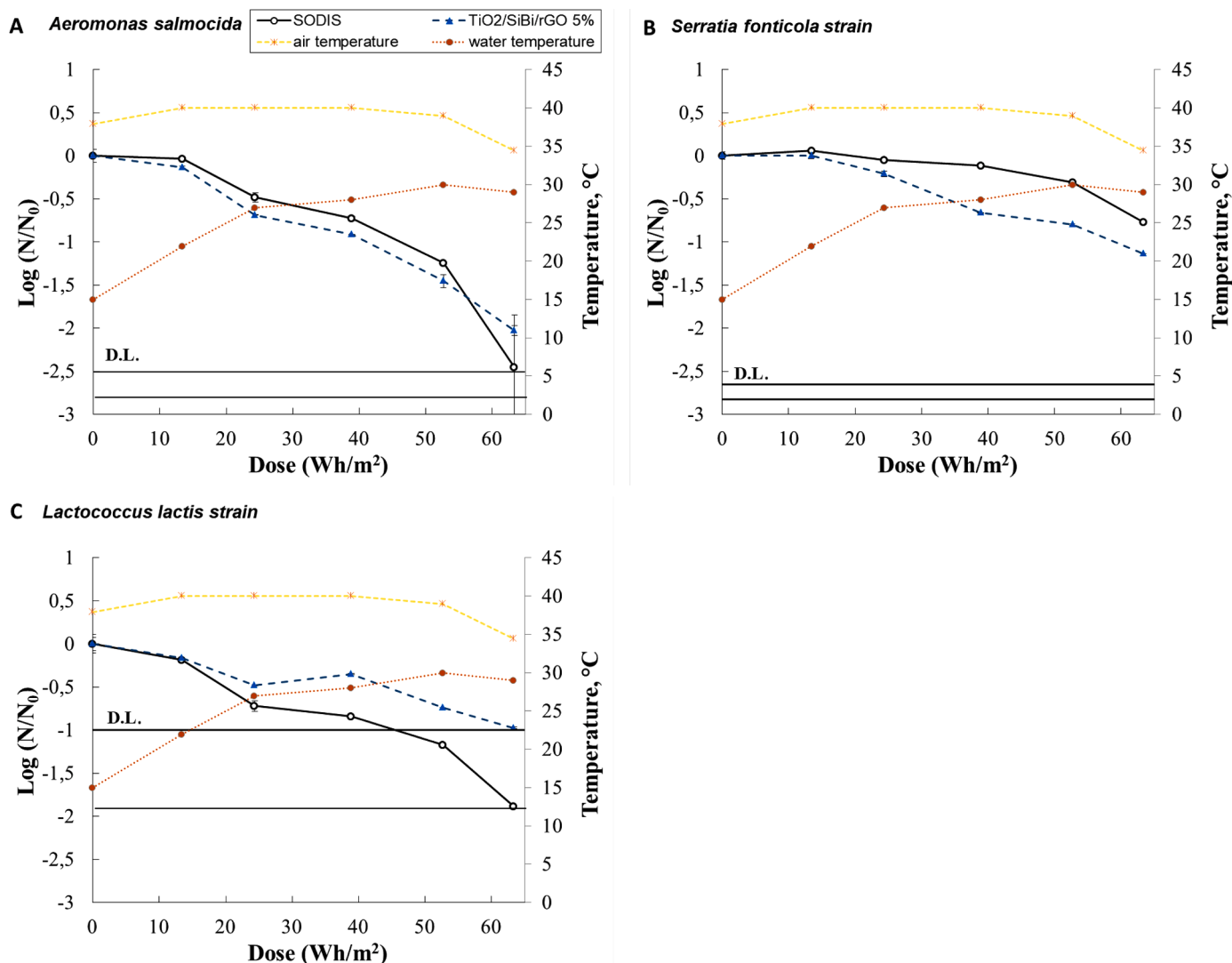


Fig. 8. Results of solar-driven photocatalytic inactivation of microorganisms in RAS stream water. A – *Aeromonas salmocida*, B – *Serratia fonticola strain*, C – *Lactococcus lactis strain*.

[73], respectively. In case of *Aeromonas salmocida* and *Serratia fonticola* strain optimal temperature partially coincides with the water temperature measured during SODIS and solar photocatalysis. Thus, it can be suggested that synergetic effect typical for SODIS did not occur as the water temperature was in the interval of optimal growth of *Aeromonas salmocida*, which means that water temperature could accelerate bacterial growth and thus decelerate disinfection. Vivar and co-authors [69] have reported that when water temperature was in the range of values close to optimal growth temperature of studied microorganism SODIS was decelerated. Similar results were reported by Giannakis et al. [74].

Comparing observed results, it can be suggested that more susceptible microorganisms for SODIS were (starting from more susceptible): *Lactococcus lactis* strain > *Aeromonas salmocida* > *Serratia fonticola* strain, while the following order can be observed for solar photocatalysis: *Aeromonas salmocida* > *Lactococcus lactis* strain > *Serratia fonticola* strain.

Based on results obtained in this study, it should be mentioned that enhancement of microorganism's inactivation due to photocatalysis with TiO₂/SiBi flexible thin films modified with reduced graphene oxide was not significant, especially when compared with SODIS. However, it should be mentioned that reactor geometry and low surface area of photocatalyst in form of thin film can be of crucial importance. Thus, it has previously been reported that TiO₂ immobilized on reactor wall can lead to decrease of solar photocatalytic disinfection in comparison with SODIS due to competition for photon absorption [65], while fixed-bed reactors with TiO₂ deposited on packing materials can be almost as effective as slurry reactors. Taking into account the cost of preparation of such coatings reported in our previous study [17], it can be suggested that further improvement of reactor geometry is and photocatalytic activity is required in order to make this process feasible.

4. Conclusions

In this study, photocatalytic inactivation of microorganisms naturally occurring in RAS stream water was studied under UVA and natural solar irradiation using printed TiO₂/SiBi flexible thin films modified with graphene oxide. Main findings are shown below:

- Reduction of graphene oxide within printed TiO₂/SiBi was observed under UVA and natural solar irradiation when coatings were placed in RAS water. It was suggested in other studies that antibacterial activity of titanium dioxide and graphene oxide composites can increase by factor 7.5 after prolong time under UV irradiation (due to GO reduction) [36]. In our study, fresh thin films were used for each experiment, thus it was not tested if photocatalytic bacteria inactivation could be improved after longer exposure to UVA or solar light. However, we have observed that after 30 min of exposure to UVA and solar light the strong color change was observed in tested coatings, which suggest that GO reduction was achieved in first 30 min of each photocatalytic test.
- Effect of rGO concentration in TiO₂/SiBi thin films on inactivation of *Citrobacter gillenii* and *Aeromonas hydrophila* was studied under UVA. The highest photocatalytic activity was observed for rGO 1 and 5%.
- Photocatalytic inactivation of *Aeromonas salmocida* and *Serratia fonticola* strain were slightly higher when rGO/TiO₂/SiBi 5% was used under natural solar light, while opposite was observed in case of *Lactococcus lactis* strain.

Generally, based on observed results it can be concluded that printed flexible rGO/TiO₂/SiBi can be promising for inactivation of microorganisms in aquaculture water. However, more studies are needed in order to understand better effect of in situ GO reduction and its effect on antimicrobial activity of coatings.

Declaration of Competing Interest

The authors declare that they have no known competing financial

interests or personal relationships that could have appeared to influence the work reported in this paper.

Acknowledgments

Authors would like to thank Jouni Vielma from Natural Resources Institute Finland for providing RAS water and M. Shekargoftar from Masaryk University for SEM measurements. Authors express their gratitude to Arūnas Meščeriakovas from University of Eastern Finland for TEM measurements. Authors are grateful for UEF Water joint funding from Saastamoinen foundation, Olvi foundation and Wihuri foundation. This research was supported by GACR project 19–14770Y funded by Czech Science Foundation and project LM2018097, funded by the Ministry of Education, Youth and Sports of the Czech Republic. J. J. Rueda Marquez would like to thank Academy of Finland (N°322339, 2019 - 2022) and Tekniikan Edistämissäätiö (TES Foundation, Finland, grant number 6120). J. Moreno-Andrés is grateful for the financial support by the European Union under the 2014–2020 ERDF Operational Programme and by the Department of Economy, Knowledge, Business and University of the Regional Government of Andalusia. Project reference: FEDER-UCA18–108023 and Grant IJC2020–042741-I funded by MCIN/AEI/ 10.13039/501100011033 and by European Union NextGenerationEU/PRTR.

Supplementary materials

Supplementary material associated with this article can be found, in the online version, at doi:10.1016/j.cej.2022.100243.

References

- [1] Food and Agriculture Organization of the United Nations, The state of world fisheries and aquaculture 2020. Sustainability in action (2020).
- [2] A. Culot, N. Grosset, M. Gautier, Overcoming the challenges of phage therapy for industrial aquaculture: a review, *Aquaculture* 513 (2019), 734423.
- [3] J. Poore, T. Nemecek, Reducing food's environmental impacts through producers and consumers, *Science* 360 (2018) 987–992.
- [4] N. Ahmed, G.M. Turchini, Recirculating aquaculture systems (RAS): environmental solution and climate change adaptation, *J. Clean. Prod.* 297 (2021), 126604.
- [5] S. Martins, E.H. Eding, M.C. Verdegem, L.T. Heinsbroek, O. Schneider, J. Blancheton, E.R. d'Orbecastel, J. Verreth, New developments in recirculating aquaculture systems in Europe: a perspective on environmental sustainability, *Aquacult. Eng.* 43 (2010) 83–93.
- [6] R.H. Piedrahita, Reducing the potential environmental impact of tank aquaculture effluents through intensification and recirculation, *Aquaculture* 226 (2003) 35–44.
- [7] J. Blancheton, K. Attramadal, L. Michaud, E.R. d'Orbecastel, O. Vadstein, Insight into bacterial population in aquaculture systems and its implication, *Aquacult. Eng.* 53 (2013) 30–39.
- [8] R. Ben-Asher, S. Ravid, M. Ucko, M. Smirnov, O. Lahav, Chlorine-based disinfection for controlling horizontal transmission of VNN in a seawater recirculating aquaculture system growing European seabass, *Aquaculture* 510 (2019) 329–336.
- [9] M.J. Sharrer, S.T. Summerfelt, G.L. Bullock, L.E. Gleason, J. Taeuber, Inactivation of bacteria using ultraviolet irradiation in a recirculating salmonid culture system, *Aquacult. Eng.* 33 (2005) 135–149.
- [10] D. Liu, S. Behrens, L. Pedersen, D.L. Straus, T. Meinelt, Peracetic acid is a suitable disinfectant for recirculating fish-microalgae integrated multi-trophic aquaculture systems, *Aquaculture Reports* 4 (2016) 136–142.
- [11] L. Pedersen, P.B. Pedersen, Hydrogen peroxide application to a commercial recirculating aquaculture system, *Aquacult. Eng.* 46 (2012) 40–46.
- [12] D. Bögner, M. Bögner, F. Schmachtl, N. Bill, J. Halfer, M.J. Slater, Hydrogen peroxide oxygenation and disinfection capacity in recirculating aquaculture systems, *Aquacult. Eng.* 92 (2021), 102140.
- [13] J. Davidson, C. Good, C. Welsh, S. Summerfelt, The effects of ozone and water exchange rates on water quality and rainbow trout *Oncorhynchus mykiss* performance in replicated water recirculating systems, *Aquacult. Eng.* 44 (2011) 80–96.
- [14] R.K. Chhetri, A. Baun, H.R. Andersen, Acute toxicity and risk evaluation of the CSO disinfectants performic acid, peracetic acid, chlorine dioxide and their by-products hydrogen peroxide and chlorite, *Sci. Total Environ.* 677 (2019) 1–8.
- [15] M. Badiola, O. Basurko, R. Piedrahita, P. Hundley, D. Mendiola, Energy use in recirculating aquaculture systems (RAS): a review, *Aquacult. Eng.* 81 (2018) 57–70.
- [16] E. Villar-Navarro, I. Levchuk, J.J. Rueda-Márquez, T. Homola, M.Á. Morínigo, R. Vahala, M. Manzano, Inactivation of simulated aquaculture stream bacteria at low temperature using advanced UVA- and solar-based oxidation methods, *Solar Energy* 227 (2021) 477–489.

- [17] J. Moreno-Andrés, J.J. Rueda-Márquez, T. Homola, J. Vielma, M.Á. Morfiño, A. Mikola, M. Sillanpää, A. Acevedo-Merino, E. Nebot, I. Levchuk, A comparison of photolytic, photochemical and photocatalytic processes for disinfection of recirculation aquaculture systems (RAS) streams, *Water Res.* 181 (2020), 115928.
- [18] J.J. Rueda-Márquez, J. Moreno-Andrés, A. Rey, C. Corada-Fernández, A. Mikola, M.A. Manzano, I. Levchuk, Post-treatment of real municipal wastewater effluents by means of granular activated carbon (GAC) based catalytic processes: a focus on abatement of pharmaceutically active compounds, *Water Res.* 192 (2021), 116833.
- [19] J.J. Rueda-Márquez, C. Palacios-Villarreal, M. Manzano, E. Blanco, M. Ramírez del Solar, I. Levchuk, Photocatalytic degradation of pharmaceutically active compounds (PhACs) in urban wastewater treatment plants effluents under controlled and natural solar irradiation using immobilized TiO₂, *Solar Energy* 208 (2020) 480–492.
- [20] J.J. Rueda-Márquez, M. Sillanpää, P. Pocostales, A. Acevedo, M.A. Manzano, Post-treatment of biologically treated wastewater containing organic contaminants using a sequence of H₂O₂ based advanced oxidation processes: photolysis and catalytic wet oxidation, *Water Res.* 71 (2015) 85–96.
- [21] J. Rueda-Márquez, I. Levchuk, I. Salcedo, A. Acevedo-Merino, M. Manzano, Post-treatment of refinery wastewater effluent using a combination of AOPs (H₂O₂ photolysis and catalytic wet peroxide oxidation) for possible water reuse. Comparison of low and medium pressure lamp performance, *Water Res.* 91 (2016) 86–96.
- [22] P. Fernandez-Ibañez, J.A. Byrne, M.I.P. López, A. Singh, S. McMichael, A. Singhal, 8 - Photocatalytic inactivation of microorganisms in water, in: R. Boukherroub, S. B. Ogale, N. Robertson (Eds.), *Nanostructured Photocatalysts*, Elsevier, 2020, pp. 229–248.
- [23] C. Guillard, T. Bui, C. Felix, V. Moules, B. Lina, P. Lejeune, Microbiological disinfection of water and air by photocatalysis, *Comptes Rendus Chimie* 11 (2008) 107–113.
- [24] S. Helali, M.I. Polo-López, P. Fernández-Ibañez, B. Ohtani, F. Amano, S. Malato, C. Guillard, Solar photocatalysis: a green technology for *E. coli* contaminated water disinfection. Effect of concentration and different types of suspended catalyst, *J. Photochem. Photobiol. A* 276 (2014) 31–40.
- [25] S. Malato, P. Fernández-Ibañez, M.I. Maldonado, J. Blanco, W. Grnajak, Decontamination and disinfection of water by solar photocatalysis: recent overview and trends, *Catal. Today* 147 (2009) 1–59.
- [26] I. García-Fernández, I. Fernández-Calderero, M.I. Polo-López, P. Fernández-Ibañez, Disinfection of urban effluents using solar TiO₂ photocatalysis: a study of significance of dissolved oxygen, temperature, type of microorganism and water matrix, *Catal Today* 240 (2015) 30–38.
- [27] S. Malato, J. Blanco, D.C. Alarcón, M.I. Maldonado, P. Fernández-Ibañez, W. Grnajak, Photocatalytic decontamination and disinfection of water with solar collectors, *Catal. Today* 122 (2007) 137–149.
- [28] C. Sichel, J. Blanco, S. Malato, P. Fernández-Ibañez, Effects of experimental conditions on *E. coli* survival during solar photocatalytic water disinfection, *J. Photochem. Photobiol. A* 189 (2007) 239–246.
- [29] Eufinger, K., Poelman, D., Poelman, H., De Gryse, R., Marin, G.B., TiO₂ thin films for photocatalytic applications, in: S.C. Nam (Ed.), *Thin Solid Films: Process and Applications*, 2008, pp. 189–227.
- [30] A. Fujishima, T.N. Rao, D.A. Tryk, Titanium dioxide photocatalysis, *J. Photochem. Photobiol. C: Photochem. Rev.* 1 (2000) 1–21.
- [31] I. Ali, X. Mbianda, A. Burakov, E. Galunin, I. Burakova, E. Mkrtchyan, A. Tkachev, V. Grachev, Graphene based adsorbents for remediation of noxious pollutants from wastewater, *Environ. Int.* 127 (2019) 160–180.
- [32] E. Kusiak-Nejman, A.W. Morawski, TiO₂/graphene-based nanocomposites for water treatment: a brief overview of charge carrier transfer, antimicrobial and photocatalytic performance, *Appl. Catal. B: Environ.* 253 (2019) 179–186.
- [33] P. Fernández-Ibañez, M.I. Polo-López, S. Malato, S. Wadhwa, J.W.J. Hamilton, P.S. M. Dunlop, R. D'Sa, E. Magee, K. O'Shea, D.D. Dionysiou, J.A. Byrne, Solar photocatalytic disinfection of water using titanium dioxide graphene composites, *Chem. Eng. J.* 261 (2015) 36–44.
- [34] N.F. Moreira, C. Narciso-da-Rocha, M.I. Polo-López, L.M. Pastrana-Martínez, J. L. Faria, C.M. Maniaia, P. Fernández-Ibañez, O.C. Nunes, A.M. Silva, Solar treatment (H₂O₂, TiO₂-P25 and GO-TiO₂ photocatalysis, photo-Fenton) of organic micropollutants, human pathogen indicators, antibiotic resistant bacteria and related genes in urban wastewater, *Water Res.* 135 (2018) 195–206.
- [35] P. Karaolia, I. Michael-Kordatou, E. Hapeshi, C. Drosou, Y. Bertakis, D. Christofilos, G.S. Armatas, L. Sygellou, T. Schwartz, N.P. Xekoukoulotakis, D. Fatta-Kassinos, Removal of antibiotics, antibiotic-resistant bacteria and their associated genes by graphene-based TiO₂ composite photocatalysts under solar radiation in urban wastewaters, *Appl. Catal. B: Environ.* 224 (2018) 810–824.
- [36] O. Akhavan, E. Ghaderi, Photocatalytic reduction of graphene oxide nanosheets on TiO₂ thin film for photoinactivation of bacteria in solar light irradiation, *The J. Phys. Chem. C* 113 (2009) 20214–20220.
- [37] M. Bideau, B. Claudel, C. Dubien, L. Faure, H. Kazouan, On the “immobilization” of titanium dioxide in the photocatalytic oxidation of spent waters, *J. Photochem. Photobiol. A* 91 (1995) 137–144.
- [38] A.Y. Shan, T.I.M. Ghazi, S.A. Rashid, Immobilisation of titanium dioxide onto supporting materials in heterogeneous photocatalysis: a review, *Appl. Catal. A: General* 389 (2010) 1–8.
- [39] H. Barndök, D. Hermosilla, C. Han, D.D. Dionysiou, C. Negro, Á. Blanco, Degradation of 1,4-dioxane from industrial wastewater by solar photocatalysis using immobilized NF-TiO₂ composite with monodisperse TiO₂ nanoparticles, *Appl. Catal. B: Environ.* 180 (2016) 44–52.
- [40] S.J. Khan, R.H. Reed, M.G. Rasul, Thin-film fixed-bed reactor for solar photocatalytic inactivation of *Aeromonas hydrophila*: influence of water quality, *BMC Microbiol.* 12 (285) (2012) 1–13.
- [41] S.J. Khan, R.H. Reed, M.G. Rasul, Thin-film fixed-bed reactor (TFBR) for solar photocatalytic inactivation of aquaculture pathogen *Aeromonas hydrophila*, *BMC Microbiol.* 12 (5) (2012) 1–11.
- [42] G. Camera-Roda, V. Loddio, L. Palmisano, F. Parrino, Photocatalytic ozonation for a sustainable aquaculture: a long-term test in a seawater aquarium, *Appl. Catal. B: Environ.* 253 (2019) 69–76.
- [43] A.R.L. Ribeiro, N.F. Moreira, G.L. Puma, A.M. Silva, Impact of water matrix on the removal of micropollutants by advanced oxidation technologies, *Chem. Eng. J.* 363 (2019) 155–173.
- [44] J.T. Pulkkinen, T. Kiuru, S.L. Aalto, J. Koskela, J. Vielma, Startup and effects of relative water renewal rate on water quality and growth of rainbow trout (*Oncorhynchus mykiss*) in a unique RAS research platform, *Aquacult. Eng.* 82 (2018) 38–45.
- [45] I. Levchuk, T. Homola, J. Moreno-Andrés, J.J. Rueda-Márquez, P. Dzik, M.Á. Morfiño, M. Sillanpää, M.A. Manzano, R. Vahala, Solar photocatalytic disinfection using ink-jet printed composite TiO₂/SiO₂ thin films on flexible substrate: applicability to drinking and marine water, *Solar Energy* 191 (2019) 518–529.
- [46] L. Bruni, R. Pastorelli, C. Viti, L. Gasco, G. Parisi, Characterisation of the intestinal microbial communities of rainbow trout (*Oncorhynchus mykiss*) fed with *Hermetia illucens* (black soldier fly) partially defatted larva meal as partial dietary protein source, *Aquaculture* 487 (2018) 56–63.
- [47] E. Rurangwa, M.C. Verdegem, Microorganisms in recirculating aquaculture systems and their management, *Rev. Aquaculture* 7 (2015) 117–130.
- [48] C. Fernández-Álvarez, D. Gijón, M. Álvarez, Y. Santos, First isolation of *Aeromonas salmonicida* subspecies *salmonicida* from diseased sea bass, *Dicentrarchus labrax* (L.), cultured in Spain, *Aquaculture Reports* 4 (2016) 36–41.
- [49] D. Gregori, I. Benchenaa, F. Chaput, S. Therias, J. Gardette, D. Léonard, C. Guillard, S. Parola, Mechanically stable and photocatalytically active TiO₂/SiO₂ hybrid films on flexible organic substrates, *J. Mater. Chem. A* 2 (2014) 20096–20104.
- [50] T. Homola, P. Dzik, M. Veselý, J. Kelar, M. Černák, M. Weiter, Fast and low-temperature (70 °C) mineralization of inkjet printed mesoporous TiO₂ photoanodes using ambient air plasma, *ACS Appl. Mater. Interfaces* 8 (2016) 33562–33571.
- [51] M.C. Biesinger, L.W.M. Lau, A.R. Gerson, R.S.C. Smart, Resolving surface chemical states in XPS analysis of first row transition metals, oxides and hydroxides: sc, Ti, V, Cu and Zn, *Appl. Surf. Sci.* 257 (2010) 887–898.
- [52] I. Levchuk, M. Sillanpää, C. Guillard, D. Gregori, D. Chateau, S. Parola, TiO₂/SiO₂ porous composite thin films: role of TiO₂ areal loading and modification with gold nanospheres on the photocatalytic activity, *Appl. Surf. Sci.* 383 (2016) 367–374.
- [53] L. O'Hare, B. Parbhoo, S.R. Leadley, Development of a methodology for XPS curve-fitting of the Si 2p core level of siloxane materials, *Surface and Interface Analysis: An Int. J. Devoted to the Dev. Appl. Techniques for the Anal. Surfaces, Interfaces and Thin Films* 36 (2004) 1427–1434.
- [54] L. O'Hare, A. Hynes, M.R. Alexander, A methodology for curve-fitting of the XPS Si 2p core level from thin siloxane coatings, *Surface and Interface Analysis: An Int. J. Devoted to the Dev. Appl. Techniques for the Anal. Surfaces, Interfaces and Thin Films* 39 (2007) 926–936.
- [55] D.B.G. Beamson, *High Resolution XPS of Organic Polymers*, John Wiley & Sons, 1992.
- [56] S. Watcharotone, D.A. Dikin, S. Stankovich, R. Piner, I. Jung, G.H. Dommett, G. Evmenenko, S. Wu, S. Chen, C. Liu, Graphene–silica composite thin films as transparent conductors, *Nano Lett.* 7 (2007) 1888–1892.
- [57] D. Yang, A. Velamakanni, G. Bozoklu, S. Park, M. Stoller, R.D. Piner, S. Stankovich, I. Jung, D.A. Field, C.A. Ventrice Jr, Chemical analysis of graphene oxide films after heat and chemical treatments by X-ray photoelectron and Micro-Raman spectroscopy, *Carbon N Y* 47 (2009) 145–152.
- [58] R. Al-Gaashani, A. Najjar, Y. Zakaria, S. Mansour, M. Atieh, XPS and structural studies of high quality graphene oxide and reduced graphene oxide prepared by different chemical oxidation methods, *Ceram. Int.* 45 (2019) 14439–14448.
- [59] L. O'Hare, B. Parbhoo, S.R. Leadley, Development of a methodology for XPS curve-fitting of the Si 2p core level of siloxane materials, *Surface and Interface Analysis: An Int. J. Devoted to the Dev. Appl. Techniques for the Anal. Surfaces, Interfaces and Thin Films* 36 (2004) 1427–1434.
- [60] D. Yang, A. Velamakanni, G. Bozoklu, S. Park, M. Stoller, R.D. Piner, S. Stankovich, I. Jung, D.A. Field, C.A. Ventrice Jr, Chemical analysis of graphene oxide films after heat and chemical treatments by X-ray photoelectron and Micro-Raman spectroscopy, *Carbon N Y* 47 (2009) 145–152.
- [61] X. Díez-Betriu, S. Álvarez-García, C. Botas, P. Álvarez, J. Sánchez-Marcos, C. Prieto, R. Menéndez, A. De Andrés, Raman spectroscopy for the study of reduction mechanisms and optimization of conductivity in graphene oxide thin films, *J. Mater. Chem. C* 1 (2013) 6905–6912.
- [62] T.V. Cuong, V.H. Pham, Q.T. Tran, S.H. Hahn, J.S. Chung, E.W. Shin, E.J. Kim, Photoluminescence and Raman studies of graphene thin films prepared by reduction of graphene oxide, *Mater. Lett.* 64 (2010) 399–401.
- [63] G. Williams, B. Seger, P.V. Kamat, TiO₂-graphene nanocomposites. UV-assisted photocatalytic reduction of graphene oxide, *ACS Nano* 2 (2008) 1487–1491.
- [64] H. Li, W. Zhang, L. Zou, L. Pan, Z. Sun, Synthesis of TiO₂-graphene composites via visible-light photocatalytic reduction of graphene oxide, *J. Mater. Res.* 26 (2011) 970–973.
- [65] C. Sordo, R. Van Grieken, J. Marugan, P. Fernández-Ibañez, Solar photocatalytic disinfection with immobilised TiO₂ at pilot-plant scale, *Water Sci. Technol.* 61 (2010) 507–512.

- [66] B.R. Cruz-Ortiz, J.W. Hamilton, C. Pablos, L. Díaz-Jiménez, D.A. Cortés-Hernández, P.K. Sharma, M. Castro-Alferez, P. Fernández-Ibañez, P.S. Dunlop, J.A. Byrne, Mechanism of photocatalytic disinfection using titania-graphene composites under UV and visible irradiation, *Chem. Eng. J.* 316 (2017) 179–186.
- [67] F.W. Low, C.W. Lai, C.P.P. Wong, Graphene and graphene/TiO₂ nanocomposites for renewable dye sensitized solar cells, *Carbonaceous Compos. Mater.* 42 (2018) 1–33.
- [68] K.G. McGuigan, T.M. Joyce, R.M. Conroy, J.B. Gillespie, M. Elmore-Meegan, Solar disinfection of drinking water contained in transparent plastic bottles: characterizing the bacterial inactivation process, *J. Appl. Microbiol.* 84 (1998) 1138–1148.
- [69] M. Vivar, N. Pichel, M. Fuentes, Solar disinfection of natural river water with low microbiological content (10–103 CFU/100ml) and evaluation of the thermal contribution to water purification, *Solar Energy* 141 (2017) 1–10.
- [70] M. Wegelin, S. Canonica, K. Mechsner, T. Fleischmann, F. Pesaro, A. Metzler, Solar water disinfection: scope of the process and analysis of radiation experiments, *Aqua* 43 (1994) 154–169.
- [71] M.A. Rouf, M.M. Rigney, Growth temperatures and temperature characteristics of *Aeromonas*, *Appl. Microbiol.* 22 (1971) 503–506.
- [72] Y. Motarjemi, G. Moy, E. Todd, *Encyclopedia of Food Safety*, Academic Press, 2013.
- [73] J. Chen, J. Shen, C. Solem, P.R. Jensen, Oxidative stress at high temperatures in *Lactococcus lactis* due to an insufficient supply of riboflavin, *Appl. Environ. Microbiol.* 79 (2013) 6140–6147.
- [74] S. Giannakis, E. Darakas, A. Escalas-Cañellas, C. Pulgarin, The antagonistic and synergistic effects of temperature during solar disinfection of synthetic secondary effluent, *J. Photochem. Photobiol. A.* 280 (2014) 14–26.